Interface-confined mixing and buried partial dislocations for Ag bilayer on Pt(111)

Kamel Aït-Mansour,[1,2,*] Harald Brune,[2] Daniele Passerone,[1] Michael Schmid,[3] Wende Xiao,[1,4] Pascal Ruffieux,[1] Andreas Buchsbaum,[3] Peter Varga,[3] Roman Fasel,[1] and Oliver Gröning[1]

[1]*Empa, Swiss Federal Laboratories for Materials Science and Technology, 8600 Dübendorf, Switzerland*

[2]*Institute of Condensed Matter Physics, Ecole Polytechnique Fédérale de Lausanne (EPFL), 1015 Lausanne, Switzerland*

[3]*Institut für Angewandte Physik, Technische Universität Wien, 1040 Wien, Austria*

[4]*Institute of Physics, Chinese Academy of Sciences, Beijing 100190, China*

(Received 8 March 2012; revised manuscript received 5 June 2012; published 3 August 2012)

The trigonal strain-relief pattern formed by an Ag bilayer on Pt(111) is a prominent example for dislocation networks and their use as nanotemplates. However, its atomic structure has not been solved. Combining scanning tunneling microscopy, low-energy ion scattering, and x-ray photoelectron diffraction, we demonstrate that, unexpectedly, about 22% of the atoms exchange across the Ag/Pt interface, and that the partial dislocations defining the trigonal network are buried in the Pt interface layer. We present an embedded-atom-method simulation identifying the lowest energy structure compatible with all experimental findings.

DOI: 10.1103/PhysRevB.86.085404 PACS number(s): 68.55.Nq, 64.75.St, 68.37.Ef

Strain-relief patterns formed by heteroepitaxial films act as templates for the self-assembly of highly ordered nanostructure superlattices.[1] The first system where the growth kinetics has been studied is a superlattice of Ag islands grown on a trigonal network (TN) formed by two monolayers (ML) of Ag/Pt(111).[2,3] The system has been modeled by assuming a network of surface Shockley partial dislocations[4] acting as repulsive line defects and thus confining the deposited Ag adatoms into the (25×25) unit cells.[2,3] However, the topmost Ag layer of the TN has recently been shown to be nearly perfectly hexagonal; hence there are no partial dislocations at the surface.[5,6] Nevertheless, the TN exhibits remarkable template functions. Well-ordered sputter holes[5] and adsorbed organic molecules,[6–8] as well as strong spatial variations of the local work function[9] have been reported. A fundamental understanding of any template function evidently requires knowledge of its atomic structure.[10] Despite considerable efforts, a realistic atomistic model has not yet been developed for the 2 ML Ag/Pt(111) TN.

Silver on Pt(111) is a system with a particularly rich surface phase diagram. Submonolayers deposited at room temperature (RT) are pseudomorphic for islands smaller than 20 nm, whereas larger islands form surface partial dislocations.[11,12] Counterintuitively, the dislocations disappear at a full monolayer (defined as one Ag atom per Pt substrate atom), where the stress resulting from the misfit is largest. This has been related to the chemical adatom potential and to the presence of an adatom gas.[11] Further growth at RT leads to a striped phase (SP)[4,13] with pairs of partial dislocations. Upon annealing to 800 K the SP transforms into the stable TN structure.[4] Deposition of Ag submonolayers at higher temperature, or their annealing at $T > 620$ K, leads to a real mixture formed by monolayer Ag clusters embedded into the uppermost atomic substrate layer for a coverage $\Theta < 0.5$ ML and the reverse for 0.5 ML $< \Theta <$ 1.0 ML.[14] This mixing has been confirmed by CO titration[15] and He-atom scattering[16] and is confined to the uppermost layer; hence, the name "surface alloy".[17] For $\Theta \geqslant 1.0$ ML, especially for $\Theta = 2$ ML, Ag and Pt were believed to be phase separated up to the Ag desorption temperature.

In this paper we report the surprising observation that the system mixes again for 2 ML Ag in the TN structure. This mixing is confined to the atomic Ag and Pt interface layers exchanging about 22% of their atoms, enabling a gradual transition in lattice constant between the two elements. Further, we show that the partial dislocations of the TN are buried in the Pt interface layer. This significantly revises the structure models previously reported for this system.[4,18,19]

Experiments were carried out in three ultrahigh vacuum multichamber systems ($p_{\text{total}} = 3 \times 10^{-11} - 1 \times 10^{-10}$ mbar), all equipped with standard surface preparation tools and scanning tunneling microscopy (STM). The first is used for high-resolution measurements with a low-temperature STM operated at 77 K, the second combines an RT micro-STM with low-energy ion scattering (LEIS) using 1 keV He^+ ions, and the third combines an RT-STM with x-ray photoelectron diffraction (XPD). STM images have been measured in constant-current mode with tunnel voltages (V_t) referring to the sample potential. Silver has been evaporated at $p_{\text{total}} < 1 \times 10^{-9}$ mbar from an *e*-beam evaporator onto Pt(111) at RT. The Ag deposition rate has been set to 0.4 ML/min and calibrated by quartz microbalance and STM. The SP has been converted to the TN by annealing the sample at 800 K for 5 min.[4]

Silver grows on Pt(111) at 300 K in the Stranski-Krastanov mode with a critical thickness for the transition from two-dimensional to three-dimensional growth of 6–9 ML.[13] Therefore for the coverage range of interest here, the growth is layer by layer, as seen in Fig. 1(a) showing an STM image of 1.9 ML Ag. One distinguishes three rotational domains of the SP of 2 ML Ag with pairs of parallel dark lines running along the $\langle 11\bar{2} \rangle$ directions.[4,13] The second Ag layer coexists with a small vacancy island exposing the first monolayer that is imaged flat reflecting the fact that this layer is pseudomorphic.[11,20]

The atomic structure of the topmost layer of the SP is shown in Fig. 1(b). As concluded from the atomic positions marked along $\langle 1\bar{1}0 \rangle$, the Ag atoms are on equal stacking sites in the left- and right-hand domains (red dots), while in the narrow stripe in-between they are shifted by 1/3 of the interatomic distance along $\langle 11\bar{2} \rangle$ (blue dots). This is the first evidence for

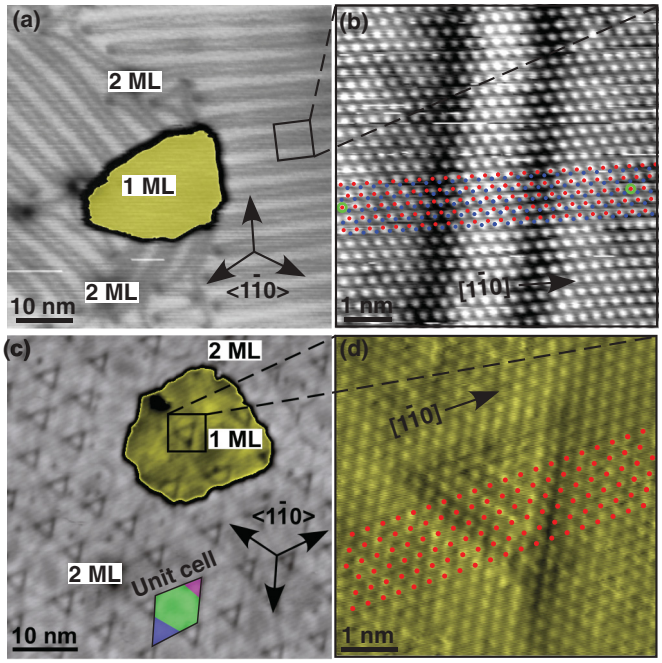

FIG. 1. (Color online) (a) STM image showing the coexistence of the 2 ML SP and the pseudomorphic 1 ML after Ag deposition on Pt(111) at RT ($\Theta = 1.9$ ML, $V_t = -1.0$ V, $I_t = 0.5$ nA, $T_{STM} = 300$ K). (b) Atomic resolution image of the SP (-5 mV, 40 nA, 77 K). (c) STM image after annealing to 800 K showing the formation of the TN on 2 and 1 ML Ag regions ($\Theta = 1.9$ ML, -2.0 V, 0.1 nA, 77 K). (d) Atomic resolution (dz/dx) image of the 1 ML Ag region shown in (c) (-40 mV, 40 nA, 77 K).

this structure having its stacking faults located in the topmost layer. The structure is $(\sqrt{3} \times n)$ with $n = 22 \pm 1$, which corrects the value $n = 14 \pm 1$ caused by a calibration error in Ref. 4. In contrast to the Au(111) herringbone reconstruction,[21] the surface partials of the SP are imaged as depressions due to buckling of underlying layers,[13] more atoms are sitting on hexagonal close-packed (hcp) than on face-centered cubic (fcc) sites (see Ref. 20 and our XPD data below), and in the SP there are 21 atoms on 22 while in Au there are 23 on 22.

An STM image of the TN is shown in Fig. 1(c). This structure has a (25×25) unit cell where the 4.3% Ag/Pt lattice mismatch can be accommodated by adsorbing 24 Ag atoms on 25 substrate atoms. The unit cell comprises a quasihexagonal region (green) and two triangular regions (purple and pink). These areas are separated by lines appearing as depressions and running along $\langle 1\bar{1}0 \rangle$. As pointed out above, and in contrast to former belief[4] and recent theory,[19] these lines are not surface partials since the topmost atomic plane is hexagonal without stacking faults [see Fig. 2(a) and Refs. 5 and 6]. Figure 1(c) shows a small vacancy island again exposing the first Ag monolayer. Instead of being pseudomorphic, this layer exhibits the TN, which is very likely induced by the surrounding 2 ML TN. The atomic-resolution STM image of the vacancy island displayed in Fig. 1(d) shows that the uppermost layer atoms form a nearly perfect hexagonal lattice without evidence of lateral displacements comparable to the expected 1/3 of the interatomic distance along $\langle 11\bar{2} \rangle$. Therefore also in the 1 ML TN the topmost Ag layer is free of partials, which hence must

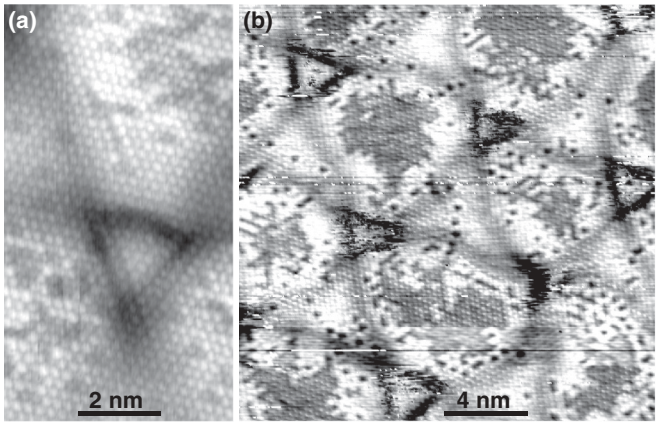

FIG. 2. STM images of the 2 ML Ag TN revealing inhomogeneities on the atomic scale (a) -10 mV, 15 nA, 77 K and (b) -1 mV, 20 nA, 300 K.

be buried in the Pt substrate, reminding one of the case of 1 ML Au/Ni(111).[22]

An additional feature of the 2 ML Ag TN is that it exhibits an intriguing STM contrast located in the quasihexagons[23] and absent on the SP. Figure 2 shows this contrast with atomic resolution, revealing that $22 \pm 2\%$ of the surface atoms appear lower by 0.15 Å.

The chemical composition of the topmost layer is addressed in LEIS measurements displayed in Fig. 3(a). The spectrum of the TN is identical to the spectra of the SP and of pure Ag taken as reference on a 7 ML Ag/Pt(111) sample. In addition, we have found very similar spectra on 1 ML Ag/Pt(111) before and after annealing to 800 K, and in both cases the Ag monolayer is found in STM to be pseudomorphic with the Pt substrate. Hence, the topmost Ag layer of all phases, 2 ML SP, 2 ML TN, and pseudomorphic 1 ML, is pure Ag. The absence of mixing for 1 ML is in agreement with earlier results.[14]

In order to investigate whether the next lower lying Ag layer of the TN contains platinum, we have used the LEIS He-ion beam to remove part of the topmost layer rendering the Ag interface layer accessible. Since the LEIS experiment itself induces mixing, we have studied as reference the SP, where Ag and Pt are known to be phase separated.[4,13] STM images reveal almost identical LEIS sputtering rates for both samples; for the chosen exposure we have removed $38.6 \pm 1\%$ ML from the TN and $34.5 \pm 1\%$ ML from the SP. The LEIS spectra obtained after removal of these amounts are shown in Fig. 3(b). They

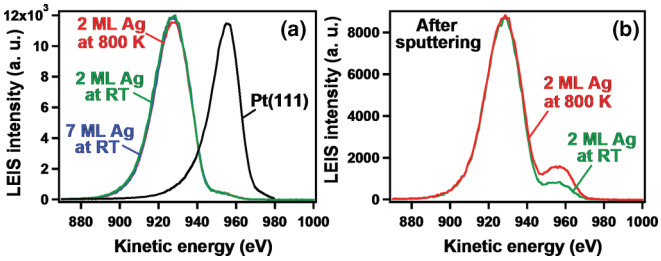

FIG. 3. (Color online) (a) LEIS spectra of 2 ML Ag/Pt(111) deposited at RT (SP), after annealing to 800 K (TN), 7 ML Ag/Pt(111) deposited at RT, and pristine Pt(111). (b) LEIS spectra after sputtering of ≈ 0.37 ML once from SP and once from TN.

exhibit in addition to the main Ag contribution a high-energy shoulder assigned to Pt atoms by comparison with the Pt(111) reference spectrum shown in Fig. 3(a). This Pt signal comes from the topmost atomic planes, and since it has been absent before removal of the topmost Ag layer, it originates from the buried Ag interface layer that therefore contains a significant fraction Pt. Part of it is caused by the LEIS measurement itself and part is intrinsic. Taking the removed Ag into account, we derive an equivalent Pt atomic concentration in the first Ag layer of $22.2 \pm 1\%$ for the SP, which determines the LEIS-induced mixing. The Pt content in the first Ag layer of the TN is with $45.5 \pm 1\%$ significantly higher. Removing the LEIS-induced mixing one arrives at an atomic Pt concentration of $23 \pm 2\%$ in the Ag interface layer of the TN. This is within the error bar identical to the concentration of Ag atoms appearing with lower height in Fig. 2(b) which identifies them as Ag atoms having Pt atoms underneath.

We have used XPD to reveal the stacking sequence and to address the question whether the Pt interface layer contains Ag. This is expected since the amount of Ag does not change upon the transformation from the SP to the TN taking place at temperatures well below the desorption threshold.[24] Figure 4 shows the Ag $3d$ core level XPD patterns from the SP (b) and TN (c) surfaces in comparison with the Pt $4f$ pattern (a). The latter has been recorded from the SP and is identical to the one from the TN. The highest intensity Ag $3d$ spots are highlighted by green circles and form triangles with identical orientation as Pt $4f$ for the TN, and inverted orientation for the SP. The peaks are due to forward focusing by topmost layer Ag atoms of $3d$ electrons emitted by Ag atoms of the underlying layer. For the SP, they show that the majority of the topmost Ag layer is hcp stacked on a pseudomorphic first Ag layer that is fcc stacked,[20,25] in full agreement with former XPD results.[20] For the TN, the strong predominance of the fcc scattering pattern for the Ag $3d$ signal is incompatible with stacking faults in the topmost two Ag layers, as in this case we should also observe a significant fraction of the XPD pattern originating from the hcp-stacked regions. This means that the stacking faults must be buried in the third lowest layer, i.e., in the Pt interface layer, as inferred from the STM results presented above.

Whether Ag mixing into the Pt interface layer takes place can be inferred from the comparison of XPD profiles with single-scattering cluster (SSC) calculations[26] displayed in Fig. 4(d). The most sensitive feature is the peak located at a polar angle of -22° and highlighted in pink. As seen in the SSC calculation of 3 ML Ag, this peak originates from Ag $3d$ emission from the third lowest layer with forward focusing along $\langle 11\bar{2} \rangle$. The height of this peak is thus a measure of the amount of Ag in this layer. The SSC calculation with 2 Ag layers and with mixed Ag and Pt interface layers, as deduced from experiment, compares well with the TN XPD profile, whereas the profile calculated for 2 ML Ag agrees best with the SP. This shows in agreement with LEIS that Ag and Pt are phase separated in the SP and more importantly it determines the layer-dependent composition of the TN: top layer clean Ag, next lower lying layer with $22 \pm 2\%$ Pt dissolved in Ag, followed by a Pt interface layer with reverse composition hosting the partials. The mixing reported here is confined to the interface since the topmost Ag layer is free of Pt, and annealing at higher temperatures leads to desorption of Ag instead of its diffusion into deeper Pt layers.[24]

Taking the experimental results into account we have simulated the atomic structure of the (25×25) unit-cell TN by means of the embedded-atom-method (EAM) classical force field[27] implemented in the program CP2K.[28] The minimum energy structure resulting from the comparison of an extended set of assumptive structures is shown in Fig. 5. These structures

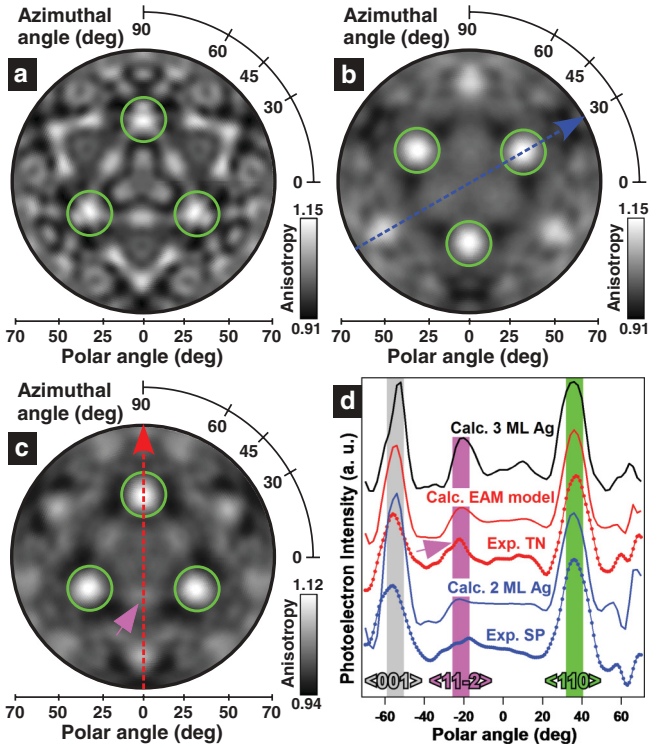

FIG. 4. (Color online) XPD patterns of (a) Pt $4f$ and (b) Ag $3d$, both from the SP, and (c) Ag $3d$ from the TN. (c) Comparison between experimental XPD profiles from the SP and TN [azimuths indicated in (b) and (c)] and SSC calculations of 2 ML Ag, of the EAM model of the TN shown in Fig. 5, and of 3 ML Ag.

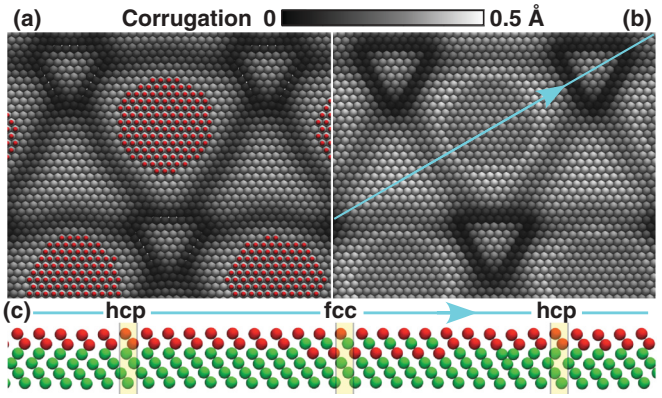

FIG. 5. (Color online) Optimized structure for the (25×25) TN as obtained by EAM calculations. (a) Pt interface layer incorporating Ag clusters highlighted in red. (b) Top Ag layer free of partials and consisting fully of Ag. (c) Cross section of the top six layers along the $\langle 11\bar{2} \rangle$ direction indicated in (b), Ag in red and Pt in green.

compare situations without intermixing or with 20% intermixing in different regions and placing the partial dislocations in different layers. As seen from Fig. 5(a) showing the Pt interface layer, the partial dislocations at the boundaries of small triangular domains are well localized, while the stacking transitions between the larger triangles and quasihexagons are spatially more extended. The incorporated Ag atoms (highlighted in red) cluster in the quasihexagonal domains. This Ag clustering generates the peak at -22° in the SSC calculation with height and shape in perfect agreement with the XPD of the TN [Fig. 4(d)]. Ag clustering in the triangular regions, or randomly distributed Ag atoms in the Pt interface layer, do not produce this agreement. The Ag interface layer, not shown here, is free of partials and contains Pt atoms assembled just above the Ag clusters embedded in the Pt interface layer. The topmost Ag layer [Fig. 5(b)], also free of partials but consisting fully of Ag, shows sharp and deep depressions around the small triangles, more shallow and spatially extended ones around the large triangles, and additional contrast centered at the quasihexagons. All these features are in perfect agreement with STM. The stacking faults in the Pt interface layer and the vertical 20% atomic exchange between the Ag and Pt interface layers in the fcc-stacked quasihexagons are clearly visible in the vertical cross section displayed in Fig. 5(c). Compared to a phase-separated structure with partials in the Pt (Ag) interface layer, this structure is lower in energy by 18.1 (21.5) meV per Pt(111) unit cell, thus naturally explaining the higher stability of the TN.

The presented structure for the TN seems to be counter-intuitive as it places the partials in the supposedly "harder" metal, i.e., the Pt, however, EAM shows that this is favored by 3.4 meV per Pt(111) unit cell with respect to partials in the Ag interface layer. For the intermixing, EAM reveals a significant energy gain of 88 meV per Ag-Pt atom pair. One of the driving forces of intermixing is that it allows a gradual adaptation of the lattice parameter from Pt bulk to the topmost Ag layer according to Vegard's law. Therefore a significant part of the energy gain comes from gradual stress relief enabled by atom exchange. We note that interface mixing has been suggested for the relaxation of the large surface stress in the present system.[29] The quantitative details of Ref. 29 had to be corrected,[30–32] however, the experimental findings presented here put these results in a new light.

In conclusion, we have studied the TN structure of 2 ML Ag/Pt(111) which forms upon annealing to 800 K. The topmost layer of the TN is pure Ag and nearly perfectly hexagonal without stacking faults. The Ag layer below contains about 22% Pt and is adsorbed on a Pt layer with the same amount of Ag and with partial dislocations. This mixing is confined to fcc-stacked regions of the immediate interface layers and creates a gradual adaptation of the lattice constant. Our findings have profound consequences on the understanding of site-specific atomic or molecular adsorption and diffusion on this surface. The former model of surface partials[4] acting as repulsive line defects[2,3] has to be revised, and the TN template is more similar to graphene or monolayer hexagonal-BN on close-packed metal surfaces, where the interaction of the topmost, defect- and dislocation-free atomic layer with the substrate leads to a spatial modulation of the adatom binding energies and diffusion barriers.

Financial support by the European Commission, the Swiss National Science Foundation, and the Austrian Science Fund (FWF) is gratefully acknowledged.

*kamel.ait-mansour@epfl.ch

[1] H. Brune, Surf. Sci. Rep. **31**, 121 (1998).
[2] H. Brune, K. Bromann, H. Röder, K. Kern, J. Jacobsen, P. Stoltze, K. Jacobsen, and J. Nørskov, Phys. Rev. B **52**, 14380R (1995).
[3] H. Brune, M. Giovannini, K. Bromann, and K. Kern, Nature (London) **394**, 451 (1998).
[4] H. Brune, H. Röder, C. Boragno, and K. Kern, Phys. Rev. B **49**, 2997 (1994).
[5] K. Aït-Mansour, A. Buchsbaum, P. Ruffieux, M. Schmid, P. Gröning, P. Varga, R. Fasel, and O. Gröning, Nano Lett. **8**, 2035 (2008).
[6] K. Aït-Mansour, P. Ruffieux, P. Gröning, R. Fasel, and O. Gröning, J. Phys. Chem. C **113**, 5292 (2009).
[7] K. Aït-Mansour, M. E. Cañas-Ventura, P. Ruffieux, R. Jaafar, M. Bieri, R. Rieger, K. Müllen, R. Fasel, and O. Gröning, Appl. Phys. Lett. **95**, 143111 (2009).
[8] K. Aït-Mansour, M. Treier, P. Ruffieux, M. Bieri, R. Jaafar, P. Gröning, R. Fasel, and O. Gröning, J. Phys. Chem. C **113**, 8407 (2009).
[9] P. Ruffieux, K. Aït-Mansour, A. Bendounan, R. Fasel, L. Patthey, P. Gröning, and O. Gröning, Phys. Rev. Lett. **102**, 086807 (2009).
[10] M. Schmid, G. Kresse, A. Buchsbaum, E. Napetschnig, S. Gritschneder, M. Reichling, and P. Varga, Phys. Rev. Lett. **99**, 196104 (2007).
[11] K. Bromann, H. Brune, M. Giovannini, and K. Kern, Surf. Sci. **388**, L1107 (1997).
[12] J. C. Hamilton, R. Stumpf, K. Bromann, M. Giovannini, K. Kern, and H. Brune, Phys. Rev. Lett. **82**, 4488 (1999).
[13] H. Röder, K. Bromann, H. Brune, and K. Kern, Surf. Sci. **376**, 13 (1997).
[14] H. Röder, R. Schuster, H. Brune, and K. Kern, Phys. Rev. Lett. **71**, 2086 (1993).
[15] U. Strüber and J. Küppers, Surf. Sci. **294**, L924 (1993).
[16] P. Zeppenfeld, M. A. Krzyzowski, C. Romainczyk, R. David, G. Comsa, H. Röder, K. Bromann, H. Brune, and K. Kern, Surf. Sci. **342**, L1131 (1995).
[17] J. Tersoff, Phys. Rev. Lett. **74**, 434 (1995).
[18] W. L. Ling, J. C. Hamilton, K. Thürmer, G. E. Thayer, J. de la Figuera, R. Q. Hwang, C. B. Carter, N. C. Bartelt, and K. F. McCarty, Surf. Sci. **600**, 1735 (2006).
[19] R. Pushpa, J. Rodríguez-Laguna, and S. N. Santalla, Phys. Rev. B **79**, 085409 (2009).
[20] G. Rangelov, T. Fauster, U. Strüber, and J. Küppers, Surf. Sci. **331–333**, 948 (1995).
[21] J. V. Barth, H. Brune, G. Ertl, and R. J. Behm, Phys. Rev. B **42**, 9307 (1990).
[22] J. Jacobsen, L. P. Nielsen, F. Besenbacher, I. Stensgaard, E. Lægsgaard, T. Rasmussen, K. W. Jacobsen, and J. K. Nørskov, Phys. Rev. Lett. **75**, 489 (1995).

[23]H. Jödicke, R. Schaub, R. Monot, J. Buttet, and W. Harbich, Surf. Sci. **475**, 109 (2001).
[24]T. Härtel, U. Strüber, and J. Küppers, Thin Solid Films **229**, 163 (1993).
[25]C. Ratsch, A. P. Seitsonen, and M. Scheffler, Phys. Rev. B **55**, 6750 (1997).
[26]R. Fasel, P. Aebi, R. G. Agostino, D. Naumović, J. Osterwalder, A. Santaniello, and L. Schlapbach, Phys. Rev. Lett. **76**, 4733 (1996).
[27]S. M. Foiles, M. I. Baskes, and M. S. Daw, Phys. Rev. B **33**, 7983 (1986).
[28]http://www.cp2k.org.
[29]A. Grossmann, W. Erley, J. B. Hannon, and H. Ibach, Phys. Rev. Lett. **77**, 127 (1996).
[30]A. Grossmann, W. Erley, J. B. Hannon, and H. Ibach, Phys. Rev. Lett. **78**, 3587 (1997).
[31]D. J. Bottomley, Jpn. J. Appl. Phys. **37**, L603 (1998).
[32]S. Narasimhan, Phys. Rev. B **69**, 045425 (2004).